A Molecular Dynamics study on the conformational stability of PrP 180-193 Helix II Prion fragment.

M.Pappalardo[1], D.Milardi[2], C.La Rosa[1], C.Zannoni[3], E.Rizzarelli[1,2] and D.Grasso[1]

[1]*Dipartimento di Scienze Chimiche, Universita' di Catania, Viale Andrea Doria 6, 95125 Catania, Italy.*
[2]*Istituto CNR di Biostrutture e Bioimmagini- Sezione di Catania, Viale Andrea Doria 6, 95125 Catania, Italy.*
[3]*Dipartimento di Chimica Fisica ed Inorganica, Università di Bologna, viale Risorgimento 4 , 40136 Bologna, Italy.*

Keywords: Prion Helix , PrP 180-193, Molecular Dynamics, hydrophobic environment

*Corresponding author:
Fax number: ++39-95-580138
Phone number: ++39-95-7385204
e-mail: dgrasso@dipchi.unict.it

Abstract

Molecular Dynamics of PrP 180-193 has allowed us to investigate the stability of the α-helical conformation of the zwitterionic peptide (L_1) and the neutralized (L_2). In water, the helical structure of L_1, is unstable; in L_2, the α-helix breaks up in the middle at Gln186, and the two resulting connected helices are stable. The hydrophobic enviroment decreases the stability of the helical structure of L_1, this effect is more evident for L_2 for which the unfolding of the C-terminus is followed by the formation of an intramolecular hydrogen bond connecting His 187 with Thr191.

Introduction

Prion diseases constitute a heterogeneous group of sporadic, inheritable and transmissible neurodegenerative disorders affecting humans and variety of mammals. They include scrapie of sheep and goats, bovine spongiform encephalopathy (BSE) and several human diseases such as Creutzfeldt-Jakob disease, Gerstmann-Straussler-Scheinker Syndrom (GSS) and familial fatal insomnia (FFI) [1,2]. Transmissible spongiform encephalopaties have attracted in the last few years enormous scientific attention because they exemplify a novel mechanism of biological information transfer based on the transmission of protein conformation rather than on the inheritance of nucleic acid sequence [3]. According to the "protein only hypothesis", first outlined in general terms by Griffith [4] and updated in its final form by Prusiner [5,6] the infectious agent is a conformational isoform of PrP^{c} [5] a protein normally found predominantly on the outer surface of neurons [7-9]. Introduction of the abnormal Prion conformer (PrP^{sc}) into the healthy organism would result in the pathological conversion PrP^{c} -> PrP^{sc}. The conversion of PrP^{c} into PrP^{sc} occurs without any chemical modifications to the protein-molecule [10,11]. However, the two proteins have very different physical properties. PrP^{c} has a predominantly alpha-helical structure, is monomeric and readily digested by proteinase K, whereas PrP^{sc} forms highly insoluble aggregates, has a large beta-sheets structure content and shows a high resistance to proteolytic digestion [12,13]

Although there is substantial evidence that the conversion of PrP^{c} -> PrP^{sc} is a key molecular event in the pathogenesis of Prion diseases, the details of the molecular mechanism involving this remarkable conformational change is poorly understood. The normal cellular form of the Prion protein is associated with the plasma membrane via a GPI anchor [14] and a second transmembrane form of two topologies (N- or C-terminus in the ER lumen) is associated with the plasma membrane via a common transmembrane fragment comprising residues 113-135 [15-17]. Many experimental observations support the hypothesis that an abnormal interaction of specific domains of PrP with the lipid membrane might be involved in the process of conversion of PrP^{c} to PrP^{sc} [18]. To gain insights into this issue, in vitro and in vivo studies have been carried out using synthetic fragments of PrP corresponding to regions of alfa-helical structure [19,20] and monitoring their physico-chemical properties [21] and their cytotoxicity in primary neuronal cultures [22]. In particular, a peptide corresponding to the second helical region of the human Prion protein (VNITIKQHTVTTTT), PrP 180-193, has been shown to form amyloid fibrils and to possess neurotoxicity *in vitro* [23]. The present study is aimed to obtain an atomic level

insight into the mechanism of the first step of amyloid formation which consists on the formation of a PrP180-193 monomeric unit prone to be converted in a β-sheet rich structure. In particular we aim to investigate: i) the effect of the electrostatic charges at the C- and N-termini; and ii) the effect of an hydrophobic solvent, mimicking the lipid environment of the cell membrane, on the α-helix stability of PrP180-193.

Two 5-ns explicit solvent MD simulations have been carried out on the L_1 and L_2 peptides solvated in water, each starting from an ideal α-helix structure; similar simulations have been carried out in ethane.

The outcome of the MD simulations has allowed us to propose a detailed molecular mechanism of the destabilization of the α-helical PrP180-193 in water and in hydrophobic environment. In addition, the effects of the electrostatic properties of the C- and N-termini have been elucidated, highlighting, in particular, the formation of a hydrogen bond between residues Thr188 and Thr193 that drives the unwinding of the α-helix of L_2 in an hydrophobic environment. The possible consequences of these results at a biological level are briefly discussed in the light of the most recent findings suggesting a key role played by the lipid membrane in triggering abnormal conformational changes in specific Prion domains.

Computational details

MD simulations have been carried out by using the program ORAC which adopts the native amber/charm Forcefield [24-27]. Non-bond interactions have been handled using a cut-off distance of 15 Å. All the trajectories and velocities have been obtained by using the r-RESPA multiple time step integrator that makes unnecessary to resort to the SHAKE procedure [28,29]. MD simulations have been carried out in a cell of 45 x 32 x 36 Å, adopting periodic boundary conditions, in which the minimum distance between any atom from the primary protein and its periodic image is at least 20 Å.

All MD simulations have been carried out by considering explicitly the solvent molecules: in the case of water, a box of 1632 solvent molecules have been considered to give a final density of 1 gr/cm^3; for simulations in an hydrophobic environment 632 molecules of ethane have been used thus obtaining a final density of 0.3 gr/cm^3 . The temperature has been controlled by using the algorithm developed by Nose and Hoover [30]. In all the simulations, the solvated peptide initially in an α-helical conformation has been gradually heated to 300 K for 40 ps using a timestep of 1 fs in an NVT ensemble; then the system has been equilibrated for 1 ns in an NPT ensemble adopting a larger timestep of 10 fs. The simulation was stopped at 1 ns because the potential energy and volume of the system remain constant (data not shown). Finally, productive MD simulations have been performed up to 20 ns using the same conditions adopted for the equilibration step.

Results and Discussion

The complete conformational analysis of the two PrP peptides L_1 and L_2 in water and ethane along the 20 – ns explicit solvent MD simulations are reported in fig.1. The α-helical content of L_1 in ethane at the beginning of the productive simulation is about 35%. The residues Val^{180}, Asn^{181}, Ile^{182} adopt a bend structure, while the region encompassing residues from Thr^{188} to Thr^{193} is highly unstable: residues Thr^{192} and Thr^{193} are in a turn conformation, while the group of residues from Thr^{188} to Thr^{191} adopts predominantly a random-coil structure. The analysis of the conformations adopted by L_1 water is more complex: if, on one hand, the α-helical content at the beginning of the simulation is higher than in water (71% vs. 35%), it decreases after 1 ns, giving rise to an unstable conformation. Similarly to what evidenced for the simulations in ethane, the Thr^{192}, Thr^{193} and Val^{180}, Asn^{181} show a marked tendency to form turn and bend structures respectively.

The conformational analysis in water of the PrP 180-193 peptide in which the N- and C- termini electrostatic charges have been neutralized (L_2), gives an initial α-helical content of about 57%; α-helix breaks up in the middle, and in particular at residue Gln^{186}. The two resulting connected helices spanning residues Val^{181}-Lys^{185} and His^{187}-Thr^{190} are stable along all the 20 ns MD simulations. The conformation of the neutralized PrP180-193 peptide in ethane has, at the beginning of the productive MD simulation, an α-helical content of about 50%. However, only residues from Thr^{182} to Gln^{186} adopt stable conformation along the 20-ns MD simulation; residues His^{187}, Thr^{188}, Val^{189} and Thr^{190} exhibit, during the first 2ns, equilibrium between a α-helical, bend and random coil conformation; after 2ns these four residues exhibit a higher conformational plasticity and a lower α-helical content.

In order to gain more insights about the mechanisms destabilizing the α-helix of PrP180-193, we report in fig.2 the distances between the residues Val^{180}-Thr^{193}, Val^{180}-Gln^{186} and Gln^{186}-Thr^{193} for the four simulations carried out; Gln^{186} has been chosen because it is located in the middle of the peptide. In panel A of figure 2 we report these three distances for the MD simulations of L_1 in water. In particular, the end to end (Val^{180}-Thr^{193}), the end to middle (Val^{180}-Gln^{186}) and the middle to end (Gln^{186}-Thr^{193}) distances are reported. All distances are calculated from C terminal to N terminal atoms of each pair of aminoacids. These distances do not show significative variations along the 20-ns simulation. After 5 ns the distanc between Val^{180} and Gln^{186} (red line) decreases. This decrease has to be ascribed to the structural reorganization of the residue Asn^{181} and Ile^{182} which undergo a conformational transition from a bend to an α-helical structure. An opposite, but less evident effect, is observed for the sequence spanning residue from Gln^{186} to Thr^{193}(blu line): in this domain

there is a smooth increase in the Gln^{186}-Thr^{193} distance, due to the different fluctuations observed for this domain (see also fig 1 left-lower panel). As a consquence of the changes of the Val^{180}–Gln^{186} and Gln^{186}–Thr^{193} distances, the end to end (green line) distance is slight decreased after 5 ns. The same simulations carried out in ethane (figure 2B) have shown, an increase of all the three distances up to 5 ns; this is due to the presence of the hydrophobic solvent which induces the unwinding of the helices either in the region encompassing residues from N-terminus to the middle, or from the middle to the C-terminus. After 5 ns in the Val^{180}–Thr^{193},Val^{180}–Gln^{186} and Gln^{186}–Thr^{193} distances are constant, but after 10 ns there is a decrease in the Val^{180}–Gln^{186} distance, which, also according to the conformational analysis reported in fig 1, can be ascribed to a turn α-helix transition of the Asn^{181} residue. MD simulations of L_2 carried out in water have not shown significant changes of the three distances along the 6-ns. After 6 ns, the Val^{180}-Gln^{186} distance decreases, and the Gln^{186}-Thr^{193} distance increases: this is in agreement with the abserved increasing α-helical content in the region encompassing residues from Val^{180} to Gln^{186} and decrease in α-helical content involving residue Thr^{190} and Thr^{191}. The distances reported in figure 3d, relative to the MD simulation of the L_2 fragment in an ethane box show an evident change in the values of the three distances after about 3ns; in particular the Val^{180}-Thr^{193} decreases, the Gln^{186} – Thr^{193} distance increases, while the Val^{180}-Gln^{186} distance remain constant along all thr simulation. This behavior can be explained only if we suppose that after 3-ns of simulation, the whole peptide bends with a fulcrum located in the middle of the peptide Gln^{186}; after about 6 ns the unfolding of α-helix encompassing residues spanning from Gln^{186} to Thr^{193} occurs, with conseqent increase in Val^{180}-Thr^{193} distance. This remarkable conformational transition is likely to be driven by the formation of novel intra-molecular hydrogen-bonds. An analysis of all hydrogen bonds that could be possible candidates to play this role, has evidenced that the distance connecting the OH group of Thr^{191} and the carboxyl oxygen of His^{187} is compatible with the formation of an H-bond. In figure 3 we report this distance, as a function of time, for all the four simulations carried out in the present study. In the case of the zwitterionic peptide L_1 it can be noted that this distance, if we exclude some oscillations occurring at 2 ns, is compatible with the existence of an hydrogen bond in water. This observation, if compared with the conformational analysis reported in figure 2, would suggest that the formation of this hydrogen bond is somehow linked to the destabilization of the α-helix at residues from Thr^{188} to the Thr^{193}. The some distance, monitored for the MD simulations in ethane, is constant along the entire simulations; on the other hand the residues His^{187} and Val^{189}, adopts predominantly an α-helical along the entire simulation.

MD simulations of the neutral peptide L_2 in water have evidenced that the distance between His^{187}-O….H-Thr^{191} is high and it is not compatible with the formation of any H bond. On the other hand we have yet evidenced that in this case the α-helical structure breaks up in the middle (see figure 2) and precisely at Gln^{186}, but the stability of these two parts in α-helix in maintained over the entire simulation. Finally, the neutral peptide L_2 in ethane exhibits, at 3-ns, a decrease of the end to end distance between Val^{180}-Thr^{193} distance (see figure 2): these charges are accompanied by a concomitant decreases of the His^{187}-O….H-Thr^{191} distance as reported in figure 3, which is diagnostic of the formation of an hydrogen bond. It is interesting to remark here that this event is also accompanied by a destabilization of the α-helix encompassing residues from Gln^{186} to Thr^{193}.

Conclusions

MD simulations of the prion fragment PrP180-193, have allowed us to evidence the followings: i) the electrostatic charges, normally presents at the C and N termini in the peptide might have noticeable effects on the helix propensity of the fragment either in water or in hydrophobic environment. In particular the part of α-helix that appears to be more sensitive to the presence of the charges at the end groups is the region encompassing residues from Thr^{188} to Thr^{193}; ii) the hydrophobic solvent has an evident effect on the helix stability of the neutral peptide; the unfolding of the α-helix comprised by residues $Gln^{186}\rightarrow Thr^{193}$ is also accompanied by a subsequent formation of an hydrogen bond between the carboxyl oxygen of His^{187} and the OH group of Thr^{191}. The formation of this hydrogen bond occurs simultaneously to the bending of entire peptide, and is a reasonable candidate to be the driving force of this curvature.

Although aware of the limits that this simplified molecular model might have if applied in the understanding of biological events, still our findings provide molecular details about the first steps triggering an abnormal conformational transition in the second helical region of the Prion molecule. The possible biological implications of the present results acquire more relevance by considering that an abnormal interaction of the prion protein with the membrane is considered one of first causes of the cascade of molecular events involved in the $PrP^{c} \rightarrow PrP^{sc}$ conversion, and, implicitly in the destabilization of the helical content of the prion protein. Moreover, the strategy proposed in the present paper, might be helpful, at an increased level of complexity of the models, in designing drugs acting as templates for "blocking" the formation of specific of H bonds which, on turn, could drive the peptide to adopt abnormal conformation

Acknowledgements

This work was partially supported by- Ministero dell'Università e della Ricerca Scientifica e Tecnologica (MIUR) (Grants: MM03194891 and 9903032282), firb RBNE01ZK8F. and Università degli studi di Catania.

References :

[1] D.A. Harris, Clin. Microbial. Rev. 12 (1999) 429.

[2] S.B. Prusiner, Proc. Natl. Acad, Sci. USA 95 (1998) 13363.

[3] T. Alper, W.A. Cramp, D.A. Haig and M.C. Clarke, Nature, 214 (1967) 764.

[4] J.S. Griffith, Nature 215 (1967) 1043.

[5] S.B. Prusiner, Annu. Rev. Microbiol. 43 (1989) 345–374.

[6] S.B. Prusiner, Philos. Trans. R. Soc. Lond. B Biol. Sci. 339 (1993) 239.

[7] B. Ocesh, D. Westaway, M. Walchli, M.P. Mc Kinley, S.B. Kent, R. Aebersold, R.A. Bazzy, P. Tempst, D.B. Teplow, L.E. Hood, S.B. Prusiner and C. Weissmann, Cell 40 (1985) 735 .

[8] B. herebro, R. Ace, K. Ahrly, J. Ischio, M. Loom, D. Lechner, S. Bergstrom, K. Robbins, L. Mayer, J.M. Keith, C. Garom, and A. Haase, Nature 315 (1985) 331.

[9] K. Basler, B. Oesch, M. Scott, D. Westway, M. Walchli, D.F. Groth, M.P. Mc Kinley, S.B. Prusiner and C. Weissmann, Cell 46 (1986) 417.

[10] B. Congtey And G.J. Raymond ,J. Biol. Chem. 266 (1991) 18217.

[11] N. Sthal, M.A. Boldein, D.B. Teplow, L. Hood, B.W. Gibson, A.L. Burlingame and S.B. Prusiner, Biochemistry 32 (1993) 1991.

[12] B. Oesch, D. Westway, M. Walchli, M.P. Mc Kinley, S.B.H. Kent, R. Aebersold, R.A Barry, P.Tempst, D.B. Teplow, L.E. Hood, S.B. Prusiner, C. Weissmann, Cell 40 (1985) 735.

[13] K.M. Pan, M.A. Boldevin, J. Nguyen, M. Gasset, A. Seruben, D. Groth, I. Mehlhorn, Z. Huang, R.J. Fletterick, F.E. Cohen, S.B. Prusiner, Proc. Natl. Acod. Sci. USA. 90 (1993) 10962

[14] N. Sthal, D.R. Borclet, K. Hsiao and S.B. Prusiner, Cell 51 (1987) 229.

[15] B. Hay, R.A. Barry, I. Llieberburg, S.B. Prusiner and V.R. Lingappa, Mol Cell. Biol. 7 (1987) 914.

[16] C.D. Lopez, C.S. Yost, S.B. Prusiner, R.M. Myers, V.R. Lingappa V.R., Science 248 (1990) 226.

[17] B. Hay, S.B. Prusiner. and V.R. Lingappa, Biochemistry 26 (1987) 8110.

[18] N. Sanghera and T.J.T. Pinheiro, J. Mol.Biol. 315 (2002) 1241.

[19] F. Lopez – Garcia, R. Zahn, R. Riek and K. Wutrich, Proc. Natl. Acad. Sci. USA 97 (2000) 8334.

[20] R. Zhan, A. Liu, T, Luhrs, C. Von Schrotter, F. Lopez – Garcia, M. Billetter, L. Calzolai, G. Wider and K. Wutrich, Proc. Natl. Acad. Sci. USA 1997 (2000) 145.

[21] M. Gasset , M.A. Boldewin, D.H. Lloyd, J.M. Gabriel, D.M. Holtzman, F.E. Cohen, R. Fletterich and S.B. Prusiner, Proc. Natl. Acad. Sci. USA 899 (1992) 10940.

[22] A. Thompson, A.R. White, C. Mc Lean, C.L. Masters, R. Cappai and C.J. Barrow, J. Neur. Res. 62 (2000) 293.

[23] D.R. Brown. V. Guantieri, G.Grasso, G. Impellizzeri, G. Pappalardo, E. Rizzarelli, J. Inorg. Chem., 98 (2004) 133.

[24] P. Procacci, T. Darden, M. Marchi., J. Phys. Chem. 100 (1996) 10464.

[25] P. Procacci, E. Paci, T. Darden, M. Marchi., J. Comp. Chemistry 18 (1997) 1848.

[26] M. Marchi, P. Procacci., J. Chem. Phys. 109 (1998) 5194.

[27] P. Procacci, M. Marchi., 1998, Proceedings of the NATO-ASI School of Erice

[28] M.E. Tuckermann, B.J. Berne, G.J. Martyna, J. Chem. Phys. 97 (1992) 1990.

[29] G.Ciccottiand, J.P.Ryckaert, Comp. phys. Report 4 (1986) 345.

[30] S. Nosé, Molec. Phys. 52 (1984) 255.

Figure captions

Fig. 1
Secondary structure as a function of simulation time for L_1 in water (left-upper panel) and in ethane (left-lower panel) and for L_2 in water (right-upper panel) and in ethane (right-lower panel). The α-helix is shown in red, the turn in green, the bend in blue and the random coil in cyano.

Fig. 2
End to end distances Val^{180}-Thr^{193} (green), Val^{180}-Gln^{186} (red line) and Gln^{186}-Thr^{193} (blu), as a function of simulation time calculated for the systems L_1/H_20 (panel A), L_1/C_2H_6 (panel B), L_2/H_20 (panel C), and L_2/C_2H_6 (panel D).

Fig. 3
Distance connecting the hydroxlylic hydrogen of Thr^{191} and the carbonil oxygen of His^{186} for the systems L_1/H_20, L_1/C_2H_6, L_2/H_20, and L_2/C_2H_6.

Fig. 4
Snapshot of the L_2/C_2H_6 system after 5-ns of MD simulation. The H-bond connecting the hydroxlylic hydrogen of Thr^{191} and the carboxyl oxygen of His^{187} is evidenced.

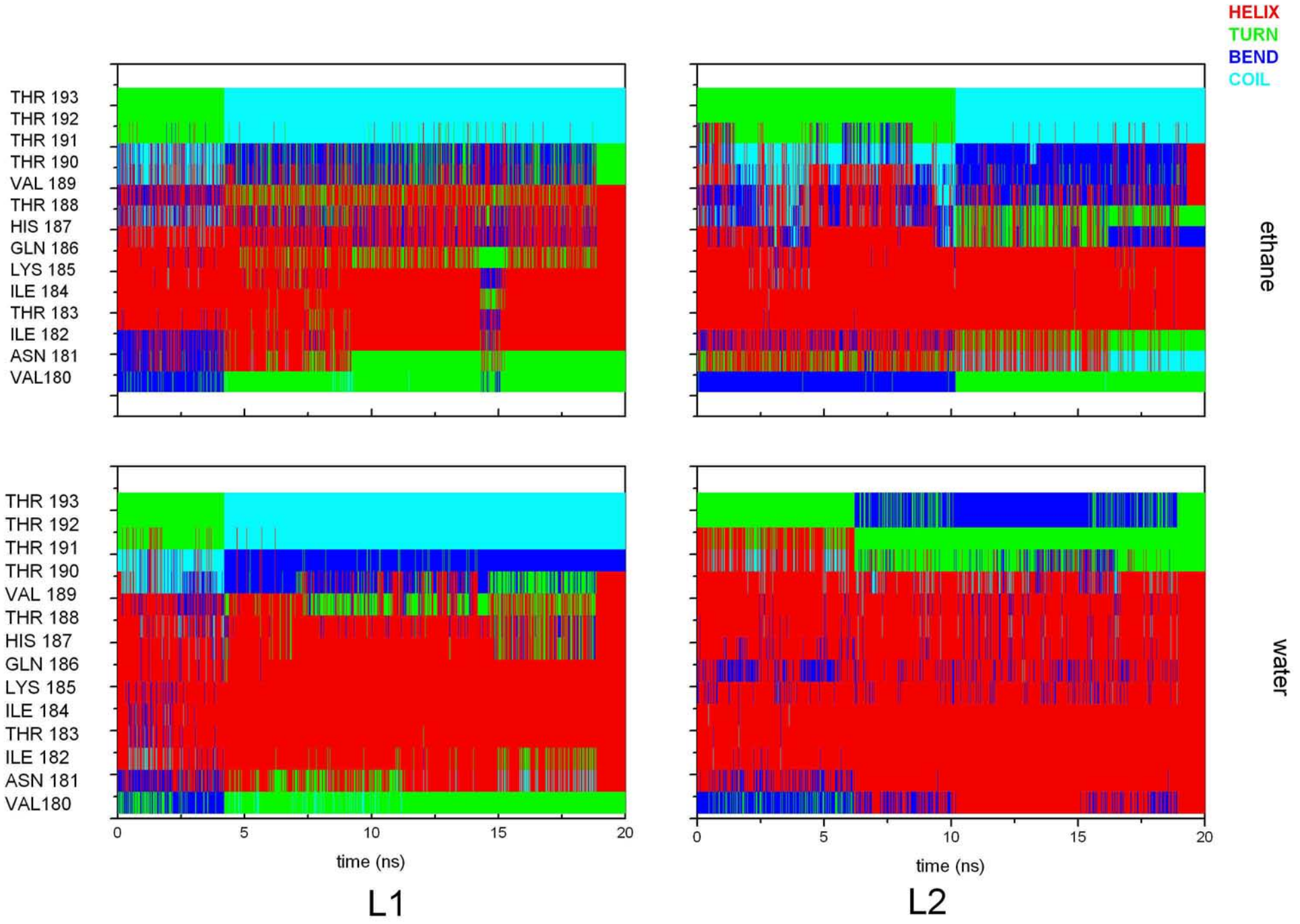
HELIX
TURN
BEND
COIL
THR 193
THR 192
THR 191
THR 190
VAL 189
THR 188
HIS 187
GLN 186
LYS 185
ILE 184
THR 183
ILE 182
ASN 181
VAL180
ethane
water
0
5
10
15
20
time (ns)
L1
L2

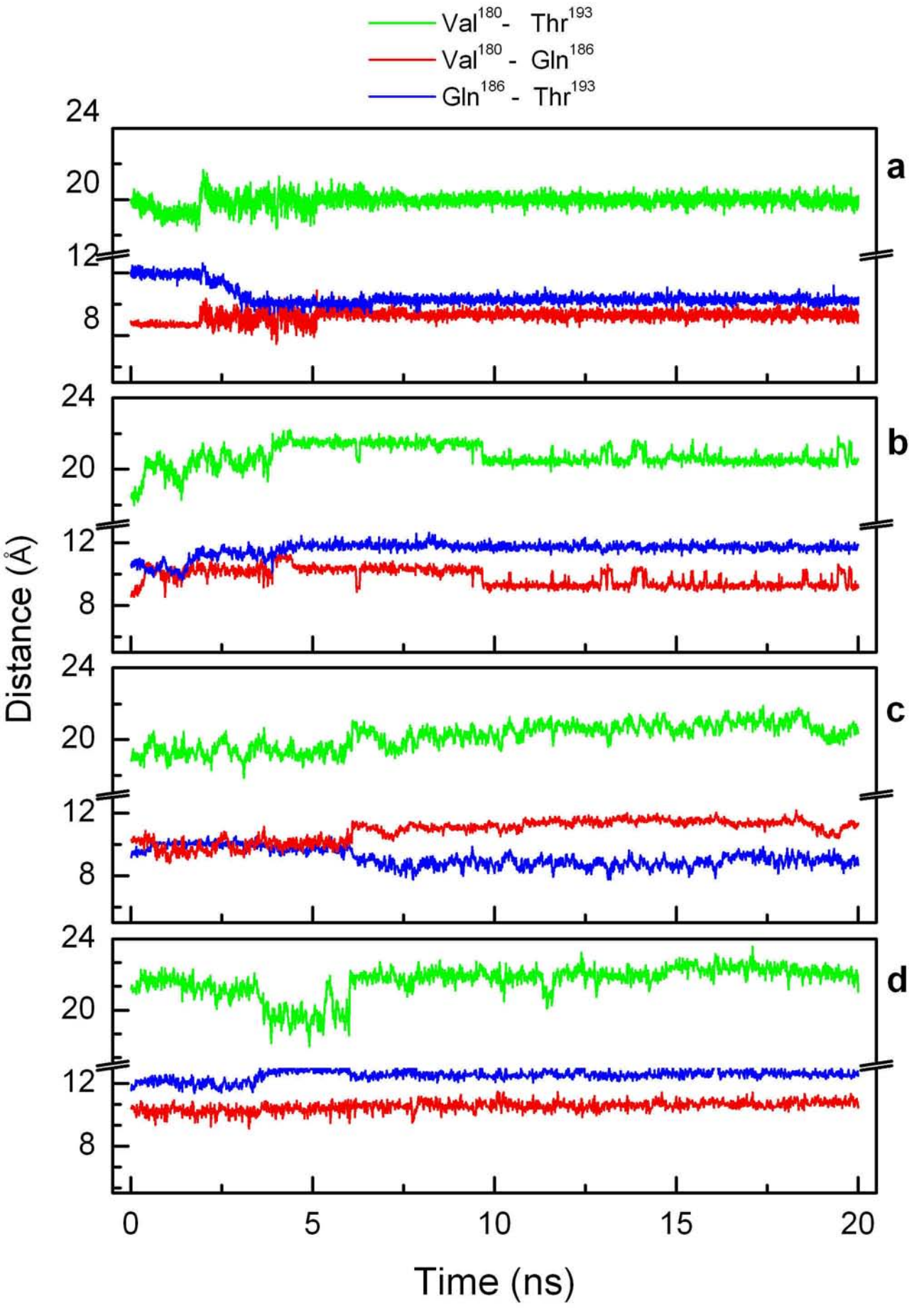
Val180- Thr193
Val180 - Gln186
Gln186 - Thr193
a
b
c
d
Distance (Å)
Time (ns)
24
20
12
8
0
5
10
15
20

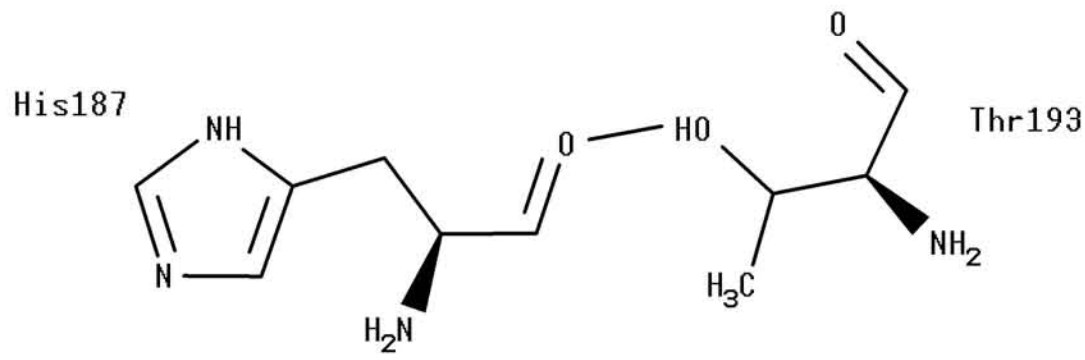
His187
NH
N
O
HO
O
Thr193
NH2
H2N
H3C

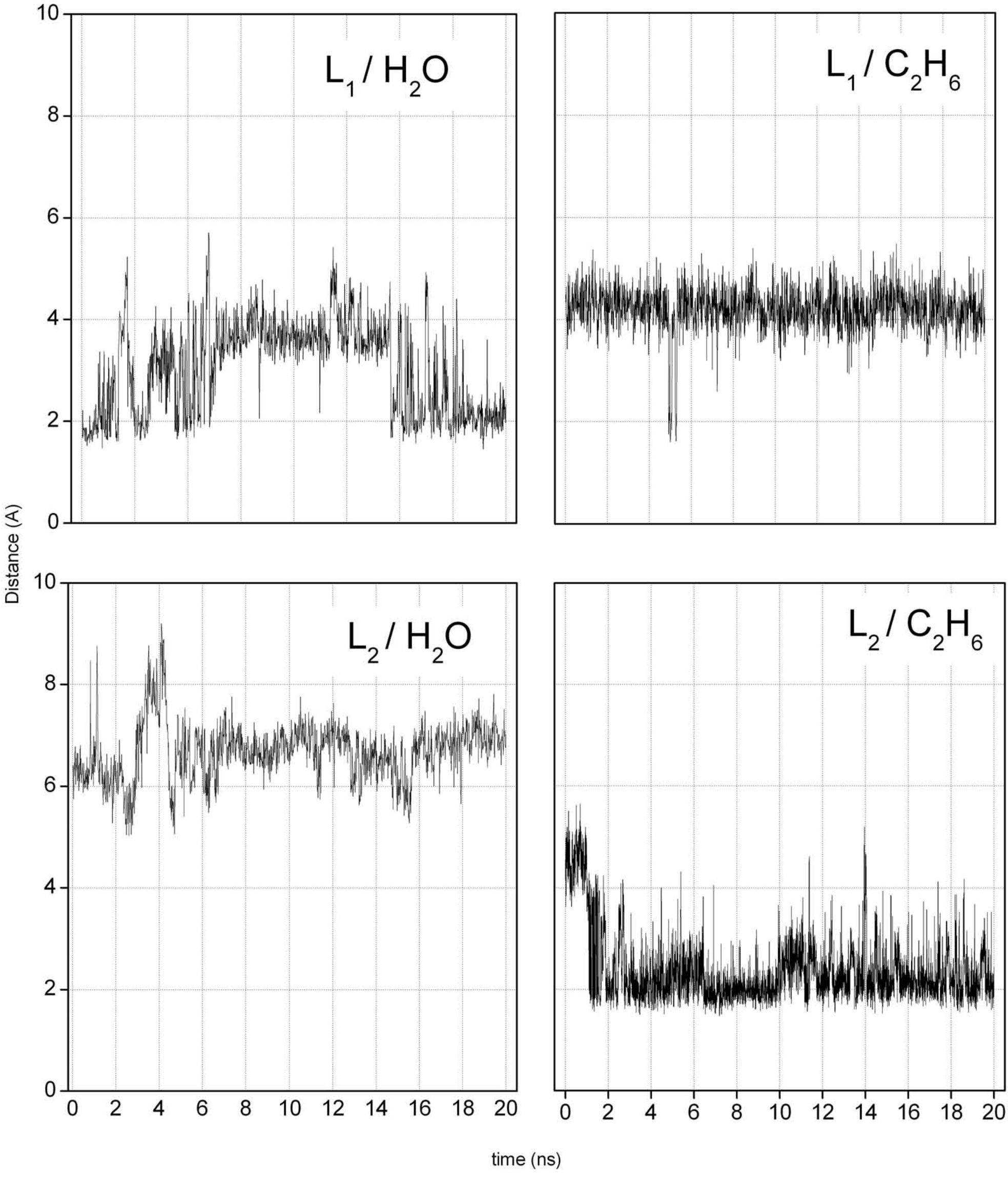
L1 / H2O
L1 / C2H6
L2 / H2O
L2 / C2H6
Distance (A)
time (ns)
0
2
4
6
8
10
12
14
16
18
20

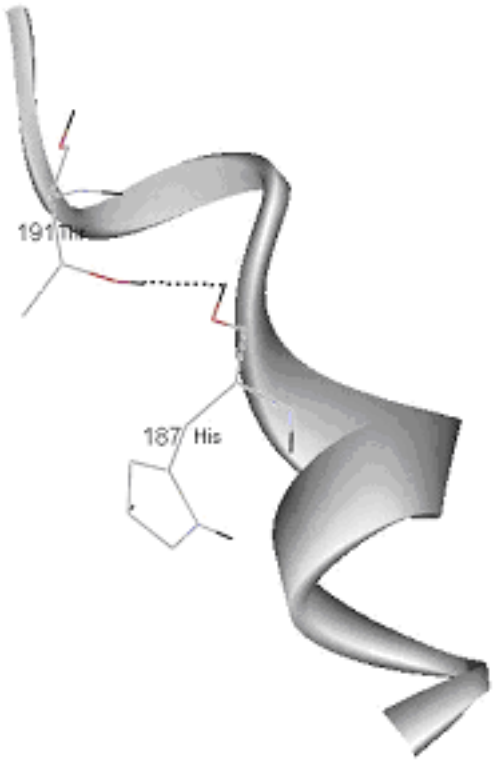

Figure 4